



## Seasonal forecasting of local-scale soil moisture droughts with Global BROOK90.

Ivan Vorobeuskii, Thi Thanh Luong, Rico Kronenberg

Faculty of Environmental Sciences, Department of Hydrosociences, Institute of Hydrology and Meteorology, Chair  
of Meteorology, Technische Universität Dresden, Tharandt, 01737, Germany

Correspondence to: Ivan Vorobeuskii ([ivan.vorobeuskii@tu-dresden.de](mailto:ivan.vorobeuskii@tu-dresden.de))

**Abstract.** Prolonged deficit of soil moisture can result in significant ecosystem and economical losses. General slowdown of vegetation growth and development, withering of foliage cover, reduction of carbon, nutrient and water cycling, increase of fire and insect outbreaks are just a few examples of soil moisture drought impacts. Thus, an early and timely warning via monitoring and forecast could help to prepare for the drought and manage its consequences.

In the study, a new version of Global BROOK90, an automated framework to simulate water balance at any location is presented. The new framework integrates seasonal meteorological forecasts from European Centre for Medium-Range Weather Forecasts (ECMWF). Here we studied how well the framework can predict the soil moisture drought on a local scale. Twelve small European catchments (from 7 to 115 km<sup>2</sup>) characterised by various geographical conditions were chosen to reconstruct the 2018-2019 period, when a large-scale prolonged drought was observed in Europe. Setting the ERA5-forced soil moisture simulations as a reference, we analysed how the lead time of the ECMWF hindcasts influences the quality of the soil moisture predictions under drought and non-drought conditions.

It was found that the hindcasted soil moisture fits well with the reference model runs only within the first (in some cases until second and third) month of lead time. Afterwards significant deviations up to 50% of soil water volume were found. Furthermore, within the drought period the ECMWF hindcast forcing resulted in overestimation of the soil moisture for most of the catchment, indicating an earlier end of a drought period. Finally, it was shown that application of the probabilistic forecast using the ensembles' quantiles to account for the uncertainty of the meteorological input is reasonable only for short-to-medium range lead times (up to three months).

### Introduction and motivation

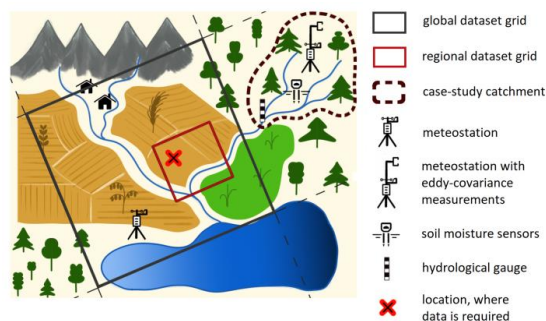
Drought is a complex, multifactorial phenomenon that includes climate, water resources, and socioeconomic factors and impacts on a community in short term as well as in long term (Crausbay et al., 2017; Grillakis, 2019; Mueller and Zhang, 2016; Sheffield et al., 2012; Wanders et al., 2014). In two past decades Europe experienced a series of dry summers with significant impacts: in 2003 (Fischer et al., 2007; Schär and Jendritzky, 2004), 2010 (Barriopedro et al., 2011), 2015 (Moravec et al., 2021; Van Lanen et al., 2016), and 2018-2020 (Moravec et al., 2021; Peters et al., 2020; Rakovec et al., 2022). The European Commission reported 9 billion euro annual monetary losses across Europe due to drought in the current situation, which will increase up to 65 billion by the end of the century for the worst climate change scenario (Naumann et al., 2021). Among commonly accepted drought types, the soil drought typically causes most of the damages for agriculture, forestry and ecosystems in general (Mishra and Singh, 2010; Sutanto et al., 2019; Zink et al., 2016). Although significant efforts are being made to develop drought monitoring and forecasting systems, the ability to forecast droughts is limited due to the



inherent uncertainties of long-term weather forecasts (Sutanto and Van Lanen, 2022; Wanders and Van Lanen, 2015). Therefore, often multiple multi-year droughts are rarely mentioned in seasonal forecasts and only reported  
40 'post factum' in observations, reports and reconstructions (Boeing et al., 2022; Boergens et al., 2020; Rakovec et al., 2022). Hence, accurate monitoring and seasonal forecasting of drought is beneficial for the development of early prevention, mitigation, and management strategies.

Recently, with the improvement of computing infrastructure and capacity, the use of probability-based seasonal weather forecasts driven by numerical weather prediction models has become more popular and advanced  
45 (Samaniego et al., 2019). This has led to the development of drought warning systems at various spatial and temporal scales (Wanders et al., 2019). Several operational monitoring and forecasting systems exist on continental, national and regional scales. These systems are principally based on rainfall, temperature and hydrological gridded observed and modelled data (Otkin et al., 2018; Sheffield et al., 2012), although new approaches such as DroughtCast (Brust et al., 2021) implementing a machine learning algorithms have also been  
50 attempted. For the United States, a real-time drought monitoring system provides information on current, short- (up to 8 weeks) and long-term (3.5 months) predicted drought conditions in 0.12° spatial resolution (Lorenz et al., 2017; Svoboda et al., 2002). It uses a combination of precipitation anomalies, evaporative stress index, soil moisture tendencies on three levels and the input of regional and local experts. The African Flood and Drought Monitor (0.25° resolution with daily updates) was developed for the monitoring purposes and provides a set of  
55 drought indexes such as SPI, soil various moisture and vegetation indices, and streamflow percentiles and deficit (Sheffield et al., 2014). Swiss monitoring and forecasting system shows canton-based current precipitation and soil moisture deficit levels as well as gives a 5- and 30-day forecast (Zappa et al., 2014). The German drought monitor (Zink et al., 2016) provides daily drought information for topsoil and full soil column based on soil moisture anomalies on a 5 km grid scale. European Drought Observatory provides up-to-date information on the  
60 occurrence and severity of droughts across Europe with 5 km resolution based on a combination of SPI, soil moisture anomaly index and vegetation greenness (Cammalleri et al., 2021), as well as basic forecasts based on SPI (Wanders et al., 2019). However, the major drawbacks of the most advanced existing frameworks is their inability to reach local-scale for the current and predicted conditions of soil moisture.

Tackling the problem of achieving high resolution in monitoring and forecasting of water balance components in  
65 general and soil moisture in particular is an ongoing process. The local scale plays a special role (Figure 1), since this is often the scale, where the final decisions are made, measures are implemented and management is taking place (European Commission, 2015; Suárez-Almiñana et al., 2017; Wagner et al., 2009). Although there are several global and national datasets, which could be used for monitoring purposes, data quality and resolution often, do not correspond to the local requirements. So far, the grid size for the state-of-the-art up-to-date global  
70 reanalysis varies in a range of 10-50 km (Gelaro et al., 2017; Ebita et al., 2011; Martens et al., 2020) and regional models can reach 1-5 km (Zink et al., 2017). Finally, even in the presence of a dense network of long-term measurements, it is highly improbable that the data of all observed variables will be available or transferable and thus representative for the desired location.



75

**Figure 1. Schematic illustration of a local scale problem in water balance estimations.**

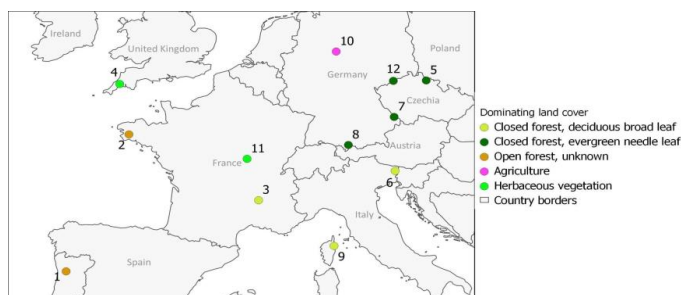
In 2020, a first version of a fully automated framework to simulate water balance in general, and soil moisture in particular on a local scale at any desired location with historical meteorological data called Global BROOK90 was released (Vorobevskii et al., 2020). The framework has thereafter been validated using runoff and evaporation components (Vorobevskii et al., 2021, 2022). Here we want to present an updated version of the framework, which  
80 integrates seasonal forecasts from the ECMWF (European Centre for Medium-Range Weather Forecasts) and thus allows long-term forecasts of the local water balance. We compare soil moisture simulations from a set of small European catchments. Therefore, we focus on the recent large European drought period using hindcast and reanalysis forcings to answer the following research questions:

- How reliable are global meso-scale seasonal forecasts as drivers of soil moisture drought simulations on a local scale?  
85
- Does the usage of ensemble quantiles advance drought prediction compared to the ensemble median or mean?

## 1. Data and Methods

### 1.1. Pilot catchments

90 For the study 12 catchments in Europe were selected (Figure 2, Table 1). The selection criteria included small catchment size, various land cover and soil types, close to natural conditions, possibly affected by the big European drought 2018-2019. Chosen catchments possess a size of 7 to 115 km<sup>2</sup> (average size 52 km<sup>2</sup>). They are covered with three different forests (opened and closed, deciduous and evergreen, needle- and broadleaf) and two short canopies types (grassland, crops) and have various soil textures. Available open-source satellite images and maps do not show significant signs of urbanisation (maximum values of 5% were identified for few catchments) or hydraulic structures (except artificial channels in cultivated areas) which could noticeably influence a natural flow regime. Although numerous reports and research of the 2018-2019 drought are available, evaluations of the drought spatial extension in 2018-19 over the Europe differ significantly (Boergens et al., 2020; Buras et al., 2020; Hari et al., 2020; JRC European Drought Observatory, 2018, 2019). However, the majority of the selected  
95 locations appear within the commonly identified territories, which were affected by the drought. The Kling-Gupta-Efficiency values for a daily scale discharge validation for the selected catchments (Vorobevskii et al., 2021) varies between 0.43 and 0.77 (with a mean of 0.57) for the evaluation time-period of 30-42 years (with a mean of  
100 38).



105

**Figure 2. Overview on the selected locations**

**Table 1. Summary on the selected catchments**

#	Name	Country	Size [km <sup>2</sup> ]	Dominating land cover types	Dominating soil texture
1	Ribeira de Sampaio - Cabriz	Portugal	10.8	Open forest (unknown), grassland	Sandy clay loam
2	Le Langelin - Brieç	France	7.04	Agriculture, grassland, open forest (unknown)	Loam
3	La Glueyre - Gluiras	France	70.9	Closed forest, deciduous broadleaf	Loam
4	Warleggan - Trengoffe	UK	25.3	Grassland, agriculture	Loam
5	Jiterka - Dolni Stepanice	Czech Republic	44.1	Closed forest (evergreen, needle leaf)	Loam
6	Ucja - Zaga	Slovenia	50.2	Closed forest (deciduous, broadleaf)	Loam
7	Grosse Ohe - Taferlruck	Germany	19.1	Closed forest (evergreen and deciduous, needle and broadleaf)	Sandy loam
8	Wertach - Wertach	Germany	34.5	Closed forest (evergreen, needle leaf)	Loam
9	Alto – Taglio-Isolaccio	France	114	Closed forest (deciduous, broadleaf)	Clay loam
10	Lenne - Oelkassen	Germany	65.6	Agriculture, closed forest (deciduous, broadleaf)	Loam
11	La Dragne - Vandenesse	France	115	Grassland, closed forest (deciduous, broadleaf)	Loam
12	Natzschung - Rothenthal	Germany	76.1	Closed forest (evergreen, needle leaf)	Sandy loam

### 1.2 Global BROOK90 v 2.0

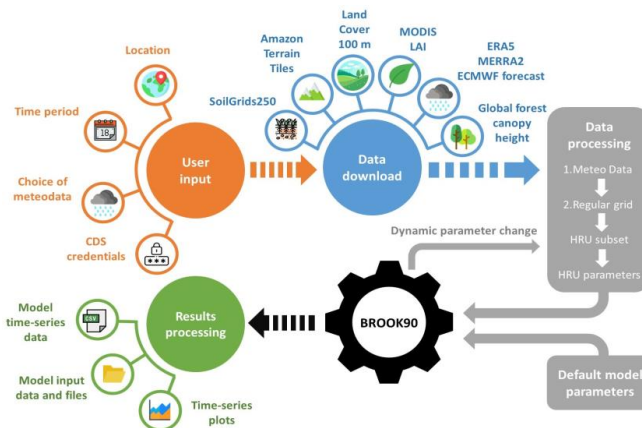
The first version of Global BROOK90 framework was introduced in 2021 (Vorobevskii et al., 2020) and the new updated version was released in 2023 (Vorobevskii, 2023a), which is applied here to simulate soil moisture. The framework uses open-source global datasets to parameterise and force the water balance model in a fully automatic mode based on the input location and time-interval.

The following datasets are incorporated to describe the characteristics of the location. For the canopy, identification and parameterization Copernicus Global land Cover 100 m (Buchhorn et al., 2020), MOD15A2H MODIS Leaf Area Index/FPAR 8-Day L4 Global (Myneni et al., 2021) and Global Forest Canopy Height (Potapov et al., 2021) are used. The SoilGrids250 dataset (Hengl et al., 2017) provides global information on soil properties for seven standard layers (texture, depth to the bedrock, stone content). Digital elevation model is downloaded from the Mapzen Terrain Tiles (Larrick et al., 2020).

For meteorological forcing, reanalysis and forecast datasets are implemented. Historical runs could be made with ERA5 (Copernicus Climate Change Service Information, 2018a) and MERRA-2 (Gelaro et al., 2017). ERA5 provides the hourly temporal and 0.25° spatial resolution data and covers the time period from 1959, while MERRA-2 has a 0.5°×0.625° grid with 6-hour time-slices and starts from 1980. For seasonal forecasting the ECMWF dataset (Copernicus Climate Change Service Information, 2018b) is integrated. It implements a 51-member ensemble meteorological forecast for 215 days on a 1° grid with daily temporal resolution and is released



on the fifth day of each month. The dataset is also available in a hindcast mode starting from 1993. For the bias-  
125 correction of the forecast, monthly simple empirical quantile mapping (Boé et al., 2007) is applied. For that, bias  
is calculated between each hindcast ensemble mean and reanalysis data on a monthly scale, and then averaged for  
each calendar month and lead time. Thereafter, the resulting bias is used to correct the forecast. Finally, Global  
BROOK90 allows combining historical and forecast simulations if the continuous timeline is preserved.  
This framework is based on the BROOK90 model (Federer et al., 2003) which is a one-dimensional physically-  
130 based model for the vertical water fluxes simulations in soil-plant-atmosphere systems. At first, the precipitation  
input goes through the canopy, where it could be either intercepted (and then evaporated) or passed through to the  
ground surface. Then, the portion reaching the ground level, could be infiltrated, frozen, evaporated, converted to  
surface flow, percolated or stored as soil moisture. The Infiltrated volume is distributed between soil layers to  
macropore bypass and matrix flow using ‘top-down’ approach. Soil water movement in the model is based on the  
135 approximations of the Richard’s equation (Richards, 1931), where the functional relationships between main soil  
parameters (soil-water content, matric potential and hydraulic conductivity) are estimated using Clapp and  
Hornberger parameterisation (Clapp and Hornberger, 1978). The soil column has groundwater, seepage and  
downslope outflow. Finally, soil water storage is used for evaporation from the top layers and root uptake for  
transpiration.  
140 The scheme of the framework is presented on Figure 3. It applies a regular 50×50 m grid to identify hydro response  
units (HRUs) based on the downloaded characteristics of the input catchment. The model is then applied separately  
to each HRU, and then an area-weighted mean for each variable is calculated from HRU output data. A more  
detailed description of the framework is presented in (Vorobevskii et al., 2020).



145 **Figure 3. Global BROOK90 framework**

As the framework aims to local scale and professional and non-professional users, it does not require substantial  
resources regarding computational power, time and memory. For example, we want to get a 7 month water balance  
forecast for a small catchment. For a test cast we can use a 4.6 km<sup>2</sup> catchment with 24 HRUs (Wernersbach Creek  
near Tharandt in Saxony, Germany) provided with the Global BROOK90 framework on GitHub. It takes around  
150 5-10 min to download elevation, land cover and soil data. Depending on requested length and type of  
meteorological data, the download time can vary from half an hour to a few days due to system build-up of  
meteorological data providers. For instance, download of one year ERA5 data for the model warm-up and 7  
months of ECMWF forecasts without hindcasts for bias correction lasted 7 hours (6 hours from which were needed



for the forecast request). Finally, computational time including data processing, modelling and saving the results  
155 on 3.4 GHz 16 GB RAM PC lasted approximately 30 min, from which the time needed to forecast one HRU with  
the abovementioned time interval yields to 1.5 min.

### 1.3 Model runs for drought 2018-2019

For the assessment of the soil moisture forecast with Global BROOK90 the time period of 2017-2020 was chosen.  
Thus, two years with 'normal' (2017, 2020) and two with 'drought' (2018-2019) conditions were considered.  
160 ERA5 with hourly resolution was used for reanalysis benchmark simulations. ECMWF hindcasts with 51  
members with daily resolution and 7 months lead time were applied for each month starting from July 2016 up to  
December 2020, so that for each month in a period of 2017-2020 all possible lead times (1-7 month) will appear.  
Additionally, for all runs one warm-up year was included. In case of a simulation with hindcast, corresponding  
ERA5 data was attached. Model input files and row simulation results are available as Supplementary  
165 (Vorobevskii, 2023b).

### 1.4 Validation of the simulated soil moisture

With the absence of available data of on-site soil moisture measurements, satellite based products were chosen  
for the validation. To benchmark the soil moisture simulations from Global BROOK90 the SMAP L4 Global 3-  
hourly 9 km EASE-Grid Surface and Root Zone Soil Moisture Geophysical Data V007 (Reichle et al., 2021a) is  
170 used. The product uses L-band brightness temperature data from satellites assimilated into a land surface model  
to estimate soil moisture on a 9 km spatial and 3 hours temporal scale globally from April 2015. The soil moisture  
is provided for the topsoil (0-5 cm), root zone (0-100 cm) and the full soil column (up to the model bedrock - e.g.  
1.3-3.8 m for the study catchments depending on specific location with a mean of 1.9 m) according to product  
description (Reichle et al., 2021b).

175 For the validation, the catchment-weighted-mean of soil moisture simulated with ERA5 was taken. As the  
thickness of standard soil layers in Global BROOK90 (dictated by SoilGrids250 dataset) does not provide a full  
match with the SMAP layout, it was decided to use the closest values of 0-2.5 cm for topsoil, 0-80 cm for root  
zone and 2 m for the whole soil profile. Since the area of one SMAP grid (81 km<sup>2</sup>) corresponds well with the sizes  
of the chosen catchments, the closest to the catchment centre grid was selected. Kling-Gupta-Efficiency (KGE)  
180 (Gupta et al., 2009) was chosen to show the agreement of volumetric water content from SMAP and Global  
BROOK90 on a monthly scale.

### 1.5 Comparison of reanalysis and forecasted soil moisture

Daily and monthly catchment-weighted mean absolute values (mm per layer) were used to compare soil moisture  
simulations using ERA5 and ECMWF forecasts. For the calculation of relative and absolute difference between  
185 ERA5 and ECMWF forcings, monthly means from the 51 forecast ensemble runs were considered. Furthermore,  
the results for topsoil (0-5 cm) and full soil column (up to 200 cm) were analysed separately. Drought periods  
were identified based on the Relative Extractable Water coefficient (Eq. 1).

$$REW = (\theta_c - \theta_{WP}) / (\theta_{FC} - \theta_{WP}) \quad (1)$$

where  $\theta$  is volumetric soil moisture at different states: C is current value at present conditions, WP is wilting point  
190 (-1500 kPa), FC is field capacity. This coefficient is calculated along with soil moisture values on a daily scale in  
Global BROOK90 and is presented in the output. Various researchers state that the values of REW below 0.2-0.4



indicate the beginning of a water stress for vegetation (Bréda et al., 2006; Granier et al., 1999; Schmidt-Walter et al., 2019; Vilhar, 2016). Here, we have chosen a threshold of 0.3 to mark drought conditions.

## 2. Results and discussion

### 195 2.1 Comparison of SMAP and ERA5-forced soil moisture

Summarised performance of Global BROOK90 with regard to SMAP data for the study catchments is shown on Figure 4. The performance of the soil moisture simulations in the upper zone of 5 cm (which in SMAP is directly assimilated from satellite data) was found better, than for the root zone and for the full profile (which in SMAP are already land surface model derivatives). The mean KGE value for the topsoil was 0.53, the lowest value 0.27  
200 was found for the catchment #8 and the highest value of 0.82 for the catchment #11. All catchments showed high correlation coefficients with a mean KGE of 0.88. However, both Global BROOK90 underestimated the mean (mean BIAS 0.82) as well as the variance (mean variance ratio 0.66) in comparison to SMAP, except for two catchments. This could be partly explained by different framework setups, namely differences in the models themselves as well as underlying datasets used to derive soil properties. With increase of the soil depth, the  
205 agreement between two datasets decreased, leading to mean KGE values of 0.48 for the root zone and 0.34 for the full column. This is mainly due to decrease of correlation and variance ratio.

Overall, the best performance was achieved for the short canopies (cultivated and herbaceous land covers), where the satellite signal could penetrate deeper through the vegetation into soil (Babaeian et al., 2019). Thus, it is not evident that Global BROOK90 simulations in tall canopies have worse performance, rather that the uncertainty  
210 of SMAP data is much higher for these land covers.

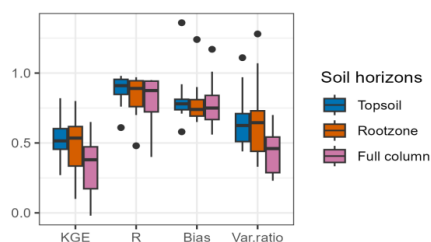


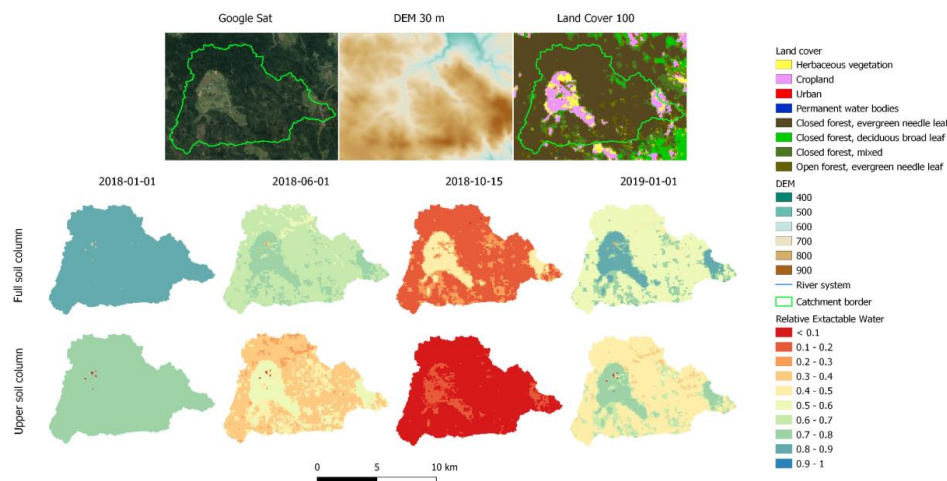
Figure 4. Kling-Gupta-Efficiency and its components between SMAP and Global BROOK90P monthly soil moisture for twelve catchments

### 2.2 Drought monitoring and forecasting on a local scale

215 Several snapshots of spatial soil water deficit for 2018 in Natzschung catchment (#12 on Figure 1) are shown in Figure 5 to show the advantages of drought monitoring with Global BROOK90 on a local scale. In January, the soil is close to saturation (REW values 0.7-0.8 for topsoil and 0.9-1 for full column). Exceptions are the few HRUs with urban areas, where the highly-sealed surfaces lead to blockage of moisture renewal. Six months later in June, when meteorological and hydrological droughts were already clearly noticeable, amounts of the soil water were  
220 reduced by around 40%, but remaining on a plant-demand level. Cultivated territories in the catchment are mainly planted with wheat, barley, oil fruits, silage maize and rye. As these cultures have a shallow effective root penetration, topsoil soil moisture (where REW values were found between 0.4 and 0.6) plays a higher role, than deeper horizons. The predominant forest species in the catchment is Norway Spruce also quite often has shallow rooting system and the majority of the root mass is concentrated in the upper soil layers (Puhe, 2003). Thus, it



225 could have already experienced some water stress by June as REW values in topsoil reached 0.2-0.4. On 15th  
 October, the minimum soil water content was observed. The upper 45 cm of soil was almost completely dry, while  
 deeper horizons under the croplands, beech and opened forests still contained plant-available soil moisture  
 (although not accessible to the crops due to root depth). As November and December brought new precipitation,  
 soil gained enough moisture for plant water supply (REW values 0.4-0.8 for topsoil and 0.5-1 for full column).  
 230 Recovery of soil moisture under the tall canopies was not as noticeable as under the short ones. This can be  
 explained with the harvesting of cultivated areas and withering on grasslands. Thus, almost no soil moisture was  
 used for transpiration, which is typically the most consumable part of water balance in this climate. Moreover, the  
 general prevailing drought conditions under the forest sites in comparison to short canopies most probably resulted  
 from much higher transpiration rates of the spruce stand. Thus, a faster depletion of soil water content is observed  
 235 there.



240 **Figure 5. Beginning, propagation and recovery of the 2018 drought on HRU scale in the Natzschung catchment for the root zone (0.45 m) and full soil column (up to 2 m).** Reference to satellite imagery: Imagery 2023 TerraMetrics, Map Data 2023, GeoBasis-DE/BKG 2009. Reference to elevation model: NASA Shuttle Radar Topography Mission Global 1 arc second, 2023. Reference to land cover map - Copernicus Global Land Service: Land Cover 100m: collection 3

The ECMWF data used as a forcing in Global BROOK90 allows getting daily ensemble predictions of soil moisture with a lead time of seven months and monthly updates. Figure 6 shows three different hindcast-forced soil moisture simulations for the Natzschung catchment. Start of each hindcast is indicated with the red dot, ensemble mean is shown with red and single ensemble runs with grey colours. In the pre-drought winter period of 2017-2018, the September hindcast ensemble mean showed approximately 10-15% underestimation of water content compared to ERA5 forcing until February. In fact, this is rather a 1-1.5 month lag due to delayed prediction of the rainy season, since the slope of the growing moisture curve as well as the saturation-plateau values look consistent between both forcings. In May 2018, when the soil moisture decline was clear according to ERA5 data, the hindcast demonstrated even a steeper depletion of water content in the first 3 months, thereafter, however, it quickly flattened out and soil moisture refill began due to significant precipitation input. Thus, ECMWF forcing not only predicted the drought recovery point two months earlier and severely overestimated soil water content by more than 25%. Finally, a hindcast started in January 2019 on the upward 'recovery' soil moisture curve showed a decent agreement with ERA5 forcing until a new seasonal decline started in April-May marking the beginning of the 2019 drought. For all the three presented hindcasts, ensemble band (especially lowest members)





255 covers the variability of ERA5 forced soil moisture through all lead times, however, a general overestimation of  
precipitation for the drought period and its variability in general in ECMWF hindcast is clear.

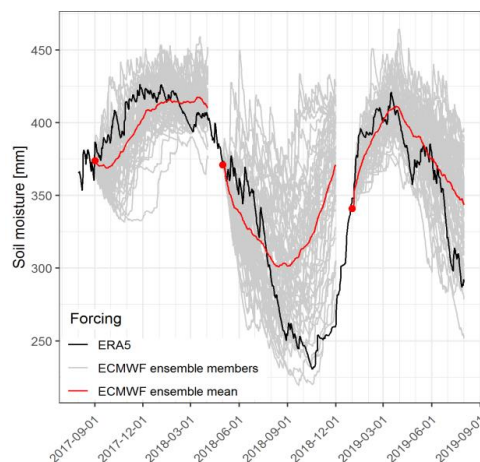


**Figure 6. Catchment-mean full-column (up to 2 m) soil moisture for the 2018 drought simulated with ERA5 and ECMWF ensemble hindcasts forcings in Natzschung**

### 260 2.3 Lead time affecting forecast accuracy

The effect of a forecast lead time in predicting the monthly soil moisture for the root zone and the full soil column in twelve selected catchments is shown in Figure 7 and Figure 8. A lead time of one month resulted in a relatively small discrepancy between hindcast and reanalysis forcings for all catchments. The relative difference rarely exceeded 10-15% (up to 20 mm) and no noticeable correlation with seasonality was observed. However, already  
265 a lead time of two (for some catchments three) months showed much higher differences (both positive and negative) between hindcast- and ERA5-forced soil moisture (up to 70% or around 150 mm). These results are consistent with similar research (Wanders et al., 2019) and indicate imperfection of meteorological input, namely increasing uncertainties of the seasonal forecasts with the growing lead time. Moreover, for the majority of the catchments (except #4) positive anomalies were found within identified drought periods ( $REW < 0.3$ ). This  
270 accounts for general overestimation of small-scale precipitation in autumn forecasts compared to ERA5. On the other hand, a big negative anomaly in August-September 2017 for catchments #2, 4, 5, 6, 10, 12 symbolises a general issue of ECMWF forecast system, which met some general problems in the whole European domain for these months. With the further increase of a lead time, the differences increase as well, however, not so drastic compared to the differences between 1 and 3 months. Thus, based on results from twelve study sites, it can be  
275 concluded that the predictability of the soil moisture using the ECMWF seasonal forecasts can be successfully accomplished with a lead time up to 2-3 months. Results for both full soil column and root zone look similar and consistent, although the difference in two datasets is more prominent for the latter one. Furthermore, it was noticed, that regardless lead time, ECMWF-forced simulations tend to show highest overestimations of the soil moisture near the end of REW-declared drought periods, thus forecasting the end of a water shortage too early,  
280 which is clearly visible for the topsoil (#1, 2, 3, 5, 6, 9, 10, 11, 12). Finally, no clear pattern between behaviour of forecasted soil moisture and catchment characteristics (i.e. dominated land cover and soil type) was found.

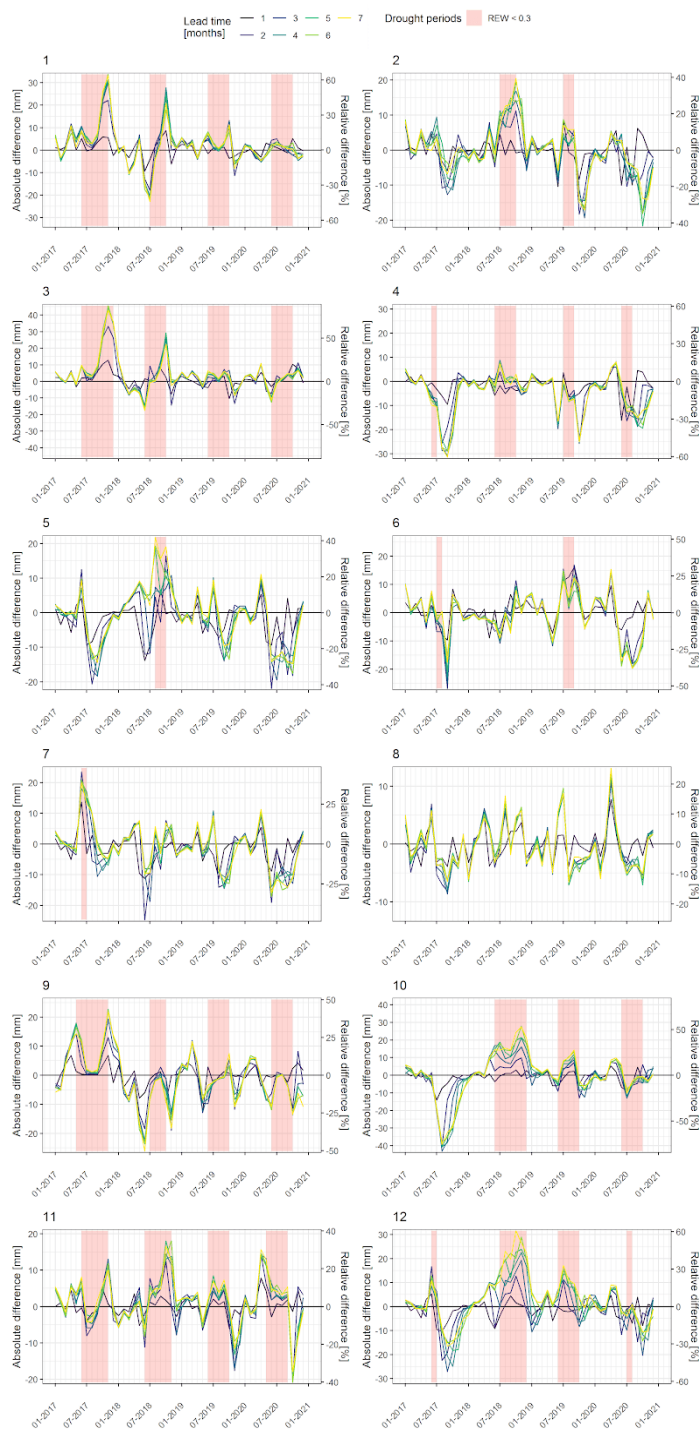
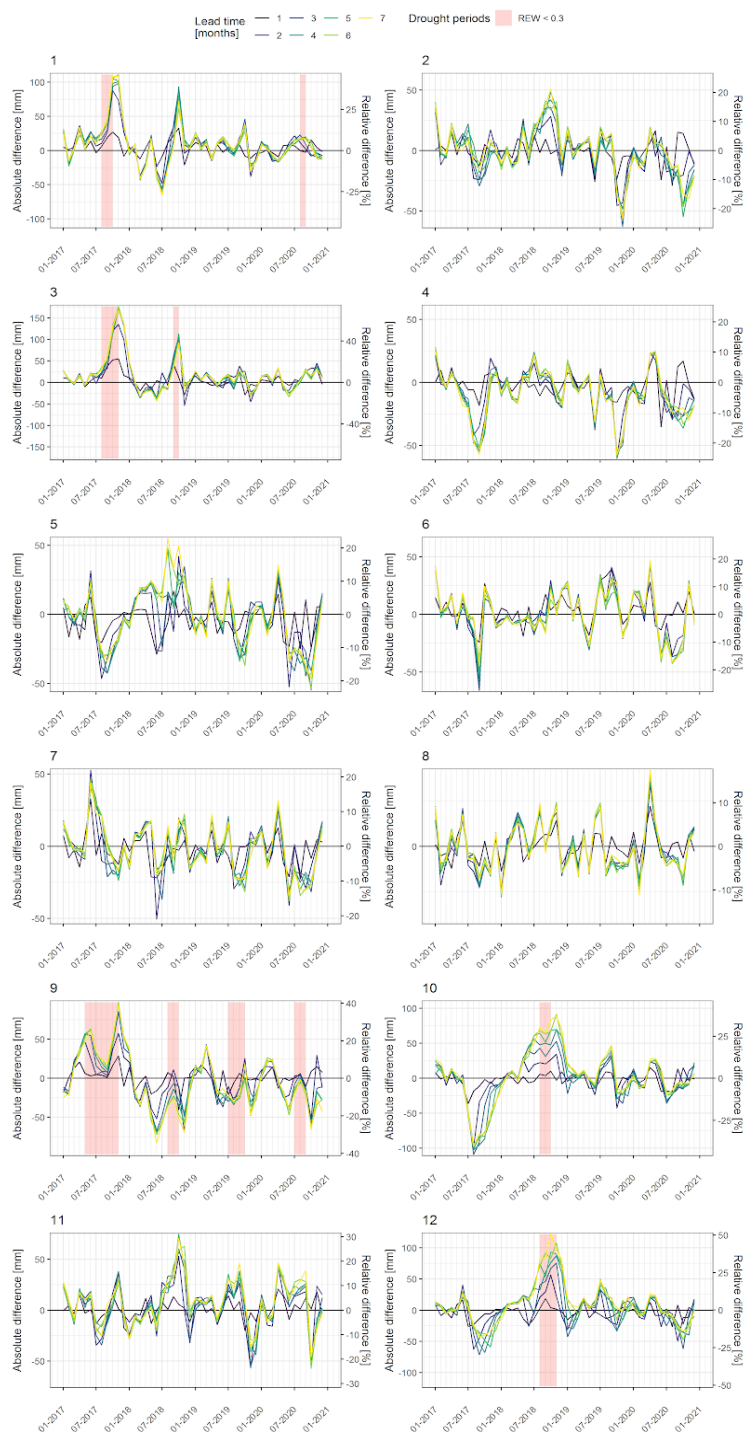


**Figure 7.** Absolute and relative difference between monthly soil moisture simulated with ECMWF hindcasts (mean of ensemble runs) and ERA5 forcings for root zone (0.45 m)



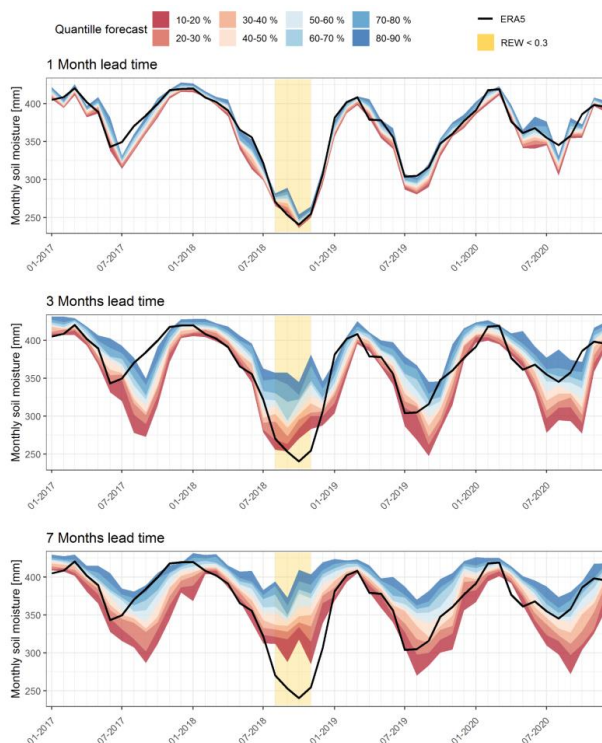
285

**Figure 8. Absolute and relative difference between monthly soil moisture simulated with ECMWF hindcasts (mean of ensemble runs) and ERA5 forcing for full soil column (up to 2 m)**



#### 2.4 Advantages of using probabilistic weather forecast

Multiple uncertainties of a weather forecast could be compensated by the advantages of using its members instead of only considering an ensemble mean. Here, the quantile predictions of monthly soil moisture simulated from 51 members of ECMWF meteorological hindcast with different lead times are presented (Figure 9). One month lead time hindcast provides a good fit with ERA5 forcing. Here the width of an ensemble band is relatively narrow due to the small uncertainty band of the meteorological conditions within a short prediction range. Minor inconsistencies in soil moisture predictions for the hindcast and ERA5 forcings (summer 2017 and 2020) probably resulted from the difference in spatial resolution between two datasets. However, already by three month lead time, the spread between ensemble mean and quantiles becomes considerable, especially in the summer period due to increased uncertainty of the meteorological forecast. Here the drought development and propagation is better depicted by lower hindcast quantiles (10-20%), while for drought attenuation in the wet season all probabilities need be used due to a delay of the drought peak in the hindcast forcing dataset. Using a 7 month lead time, thus staying on the edge of seasonal forecast predictability, will bring even a higher spread in quantile hindcasts, however with close developments as for 3 month lead time. Here, the magnitude of soil moisture drought in the 2018 cannot be captured even with 1% quantile for 5 months in a row, meaning a significant overestimation of precipitation with increasing leading time for this year.



305 **Figure 9.** Monthly averages of a catchment-mean full-column (up to 2 m) soil moisture simulated with ERA5 and ECMWF hindcasts forcings in Natzschung



### 3. Conclusion and outlook

In the article, we present a new version of an automatic framework for water balance modelling on a local scale for any location on the globe called Global BROOK90. The special focus is given on the ability of the new version to provide predictions of water balance components up to seven months in advance by incorporation of ECMWF seasonal meteorological forecasts. We showed how a combination of global open-source datasets with a physically-based model could forecast a soil moisture drought on a local scale.

Soil moisture simulations were conducted for twelve small catchments with various landscapes located in Europe within the 2017-2020 time period, which cover the well-known continent-scale European drought of 2018-2019. We used ERA5 reanalysis and ECMWF hindcasts as a meteorological forcing, where the ERA5 runs served as a reference for the soil moisture to assess the quality of the forecast performance. With an example catchment we showed spatio-temporal advantages of small-scale modelling in monitoring and forecasting a drought.

Additionally, the ERA5-forced model runs were compared with SMAP data, which represents a satellite brightness temperature assimilated in a land surface model. Validation resulted in a good agreement of both datasets on a monthly scale, especially for the correlation coefficient. However, Global BROOK90 ended up with lower mean and variance of soil moisture. Highest KGE values were found for the topsoil and the goodness of fit declined with a profile depth.

Comparison of monthly soil moisture showed that forecasts could provide acceptable results up to maximum 3 month lead time. Thereafter, the difference between two forcings could be more than 100 mm or 50% of the total soil water, which is a considerable amount, especially for the drought periods. Furthermore, it was found that for the majority of the study sites, ECMWF forecast resulted in overestimation of the soil moisture in identified plant-water-stress periods.

Finally, possible advantages of probabilistic instead of only deterministic soil moisture forecasts using quantiles of ensemble runs were assessed. It was shown that for the lead times up to three months the method could be advantageous as the band of quantile forecast could cover the variability of soil moisture produced with ERA5 forcing. However, as the hindcast-forced runs in the drought period generally tend to overestimate soil moisture and for the 7 month lead time even 10% hindcast was found insufficient to reach ERA5-forced soil moisture values.

Overall, Global BROOK90 combined with ECMWF seasonal ensemble forecasts showed good results for a mid-term range and can serve as a decent basis for drought monitoring and forecasting on a local scale. Moreover, one of the definitive advantages of the framework is that it does not require big computational resources or programming background and could be run on a normal computer or laptop by a non-professional user.

#### Data and Code availability

Authors fully support open-source and reproducible research. Global BROOK90 framework is available under [https://github.com/hydrovorobey/Global\\_BROOK90](https://github.com/hydrovorobey/Global_BROOK90) repository (CC BY-NC-ND 4.0). Simulation results, initial and simulation datasets and R-scripts to reproduce figures and tables for the manuscript are available under the following HydroShare composite resource <https://doi.org/10.4211/hs.d882e83bae95438881c7b47f003e7a3c>.



### Author contribution

Conceptualization VI and KR; data curation VI and LTT, formal analysis VI, methodology VI, LTT and KR;  
345 supervision KR; visualization VI; writing: original draft preparation VI and LTT, writing: review KR.

### Competing interests

The authors declare that they have no conflict of interest.

### Funding

Open Access Funding by the Publication Fund of the TU Dresden. This research was also funded by the German  
350 Federal Ministry of Education and Research (FKZ 01LR 2005A—funding measure “Regional Information on  
Climate Action”) (RegIKlim), section (a) Model Regions.

### References

- Babaeian, E., Sadeghi, M., Jones, S. B., Montzka, C., Vereecken, H., and Tuller, M.: Ground, Proximal, and  
Satellite Remote Sensing of Soil Moisture, *Reviews of Geophysics*, 57, 530–616,  
355 <https://doi.org/10.1029/2018RG000618>, 2019.
- Barriopedro, D., Fischer, E. M., Luterbacher, J., Trigo, R. M., and García-Herrera, R.: The Hot Summer of 2010:  
Redrawing the Temperature Record Map of Europe, *Science*, 332, 220–224,  
<https://doi.org/10.1126/science.1201224>, 2011.
- Boé, J., Terray, L., Habets, F., and Martin, E.: Statistical and dynamical downscaling of the Seine basin climate  
360 for hydro-meteorological studies, *International Journal of Climatology*, 27, 1643–1655,  
<https://doi.org/10.1002/joc.1602>, 2007.
- Boeing, F., Rakovec, O., Kumar, R., Samaniego, L., Schrön, M., Hildebrandt, A., Rebmann, C., Thober, S.,  
Müller, S., Zacharias, S., Bogena, H., Schneider, K., Kiese, R., Attinger, S., and Marx, A.: High-resolution drought  
simulations and comparison to soil moisture observations in Germany, *Hydrology and Earth System Sciences*, 26,  
365 5137–5161, <https://doi.org/10.5194/hess-26-5137-2022>, 2022.
- Boergens, E., Güntner, A., Dobsław, H., and Dahle, C.: Quantifying the Central European Droughts in 2018 and  
2019 With GRACE Follow-On, *Geophysical Research Letters*, 47, <https://doi.org/10.1029/2020GL087285>, 2020.
- Bréda, N., Huc, R., Granier, A., and Dreyer, E.: Temperate forest trees and stands under severe drought: a review  
of ecophysiological responses, adaptation processes and long-term consequences, *Ann. For. Sci.*, 63, 625–644,  
370 <https://doi.org/10.1051/forest:2006042>, 2006.
- Brust, C., Kimball, J. S., Maneta, M. P., Jencso, K., and Reichle, R. H.: DroughtCast: A Machine Learning  
Forecast of the United States Drought Monitor, *Frontiers in Big Data*, 4,  
<https://doi.org/10.3389/fdata.2021.773478>, 2021.
- Buchhorn, M., Smets, B., Bertels, L., Lesiv, M., Tsendbazar, N.-E., Herold, M., and Fritz, S.: Copernicus Global  
375 Land Service: Land Cover 100m: collection 3: epoch 2019: Globe 2020, <https://doi.org/10.5281/zenodo.3939050>,  
2020.
- Buras, A., Rammig, A., and Zang, C. S.: Quantifying impacts of the 2018 drought on European ecosystems in  
comparison to 2003, *Biogeosciences*, 17, 1655–1672, <https://doi.org/10.5194/bg-17-1655-2020>, 2020.
- Cammalleri, C., Arias-Muñoz, C., Barbosa, P., de Jager, A., Magni, D., Masante, D., Mazzeschi, M., McCormick,  
380 N., Naumann, G., Spinoni, J., and Vogt, J.: A revision of the Combined Drought Indicator (CDI) used in the  
European Drought Observatory (EDO), *Natural Hazards and Earth System Sciences*, 21, 481–495,  
<https://doi.org/10.5194/nhess-21-481-2021>, 2021.
- Clapp, R. B. and Hornberger, G. M.: Empirical equations for some soil hydraulic properties, *Water Resources  
Research*, 14, 601–604, <https://doi.org/10.1029/WR014i004p0601>, 1978.
- 385 Copernicus Climate Change Service Information: ERA5: Fifth generation of ECMWF atmospheric reanalyses of  
the global climate. ERA5 hourly data on single levels from 1959 to present, 10.24381/cds.adbb2d47, 2018a.  
Copernicus Climate Change Service Information: Copernicus Climate Change Service (C3S): Seasonal forecast  
daily and subdaily data on single levels, <https://doi.org/10.24381/cds.181d637e>, 2018b.
- Crausbay, S. D., Ramirez, A. R., Carter, S. L., Cross, M. S., Hall, K. R., Bathke, D. J., Betancourt, J. L., Colt, S.,  
390 Cravens, A. E., Dalton, M. S., Dunham, J. B., Hay, L. E., Hayes, M. J., McEvoy, J., McNutt, C. A., Moritz, M.



- A., Nislow, K. H., Raheem, N., and Sanford, T.: Defining Ecological Drought for the Twenty-First Century, *Bulletin of the American Meteorological Society*, 98, 2543–2550, <https://doi.org/10.1175/BAMS-D-16-0292.1>, 2017.
- 395 Ebita, A., Kobayashi, S., Ota, Y., Moriya, M., Kumabe, R., Onogi, K., Harada, Y., Yasui, S., Miyaoka, K., Takahashi, K., Kamahori, H., Kobayashi, C., Endo, H., Soma, M., Oikawa, Y., and Ishimizu, T.: The Japanese 55-year Reanalysis “JRA-55”: An Interim Report, *SOLA*, 7, 149–152, <https://doi.org/10.2151/sola.2011-038>, 2011.
- European Commission: Guidance document on the application of water balances for supporting the implementation of the WFD, 6.1., Office for Official Publications of the European Communities, Luxembourg, <https://op.europa.eu/en/publication-detail/-/publication/7d148604-faf0-11e5-b713-01aa75ed71a1>, 2015.
- 400 Federer, C. A., Vörösmarty, C., and Fekete, B.: Sensitivity of Annual Evaporation to Soil and Root Properties in Two Models of Contrasting Complexity, *Journal of Hydrometeorology*, 4, 1276–1290, [https://doi.org/10.1175/1525-7541\(2003\)004<1276:SOAETS>2.0.CO;2](https://doi.org/10.1175/1525-7541(2003)004<1276:SOAETS>2.0.CO;2), 2003.
- Fischer, E. M., Seneviratne, S. I., Vidale, P. L., Lüthi, D., and Schär, C.: Soil Moisture–Atmosphere Interactions during the 2003 European Summer Heat Wave, *Journal of Climate*, 20, 5081–5099, <https://doi.org/10.1175/JCLI4288.1>, 2007.
- 405 Gelaro, R., McCarty, W., Suárez, M. J., Todling, R., Molod, A., Takacs, L., Randles, C. A., Darmenov, A., Bosilovich, M. G., Reichle, R., Wargan, K., Coy, L., Cullather, R., Draper, C., Akella, S., Buchard, V., Conaty, A., da Silva, A. M., Gu, W., Kim, G.-K., Koster, R., Lucchesi, R., Merkova, D., Nielsen, J. E., Partyka, G., Pawson, S., Putman, W., Rienecker, M., Schubert, S. D., Sienkiewicz, M., and Zhao, B.: The Modern-Era Retrospective Analysis for Research and Applications, Version 2 (MERRA-2), *J. Climate*, 30, 5419–5454, <https://doi.org/10.1175/JCLI-D-16-0758.1>, 2017.
- Granier, A., Bréda, N., Biron, P., and Villette, S.: A lumped water balance model to evaluate duration and intensity of drought constraints in forest stands, *Ecological Modelling*, 116, 269–283, [https://doi.org/10.1016/S0304-3800\(98\)00205-1](https://doi.org/10.1016/S0304-3800(98)00205-1), 1999.
- 415 Grillakis, M. G.: Increase in severe and extreme soil moisture droughts for Europe under climate change, *Science of The Total Environment*, 660, 1245–1255, <https://doi.org/10.1016/j.scitotenv.2019.01.001>, 2019.
- Gupta, H. V., Kling, H., Yilmaz, K. K., and Martinez, G. F.: Decomposition of the mean squared error and NSE performance criteria: Implications for improving hydrological modelling, *Journal of Hydrology*, 377, 80–91, <https://doi.org/10.1016/j.jhydrol.2009.08.003>, 2009.
- 420 Hari, V., Rakovec, O., Markonis, Y., Hanel, M., and Kumar, R.: Increased future occurrences of the exceptional 2018–2019 Central European drought under global warming, *Scientific Reports*, 10, <https://doi.org/10.1038/s41598-020-68872-9>, 2020.
- Hengl, T., Mendes de Jesus, J., Heuvelink, G. B. M., Ruiperez Gonzalez, M., Kilibarda, M., Blagotić, A., Shangguan, W., Wright, M. N., Geng, X., Bauer-Marschallinger, B., Guevara, M. A., Vargas, R., MacMillan, R. A., Batjes, N. H., Leenaars, J. G. B., Ribeiro, E., Wheeler, I., Mantel, S., and Kempen, B.: SoilGrids250m: Global gridded soil information based on machine learning, *PLOS ONE*, 12, 1–40, <https://doi.org/10.1371/journal.pone.0169748>, 2017.
- 425 JRC European Drought Observatory: EDO Analytical Report: Drought in Central-Northern Europe – September 2018, [https://edo.jrc.ec.europa.eu/documents/news/EDODroughtNews201809\\_Central\\_North\\_Europe.pdf](https://edo.jrc.ec.europa.eu/documents/news/EDODroughtNews201809_Central_North_Europe.pdf), 2018.
- JRC European Drought Observatory: EDO Analytical Report: Drought in Europe – August 2019, [https://edo.jrc.ec.europa.eu/documents/news/EDODroughtNews201908\\_Europe.pdf](https://edo.jrc.ec.europa.eu/documents/news/EDODroughtNews201908_Europe.pdf), 2019.
- 435 Larrick, G., Tian, Y., Rogers, U., Acosta, H., and Shen, F.: Interactive Visualization of 3D Terrain Data Stored in the Cloud, in: 2020 11th IEEE Annual Ubiquitous Computing, Electronics & Mobile Communication Conference (UEMCON), 0063–0070, <https://doi.org/10.1109/UEMCON51285.2020.9298063>, 2020.
- Lorenz, D. J., Otkin, J. A., Svoboda, M., Hain, C. R., Anderson, M. C., and Zhong, Y.: Predicting the U.S. Drought Monitor Using Precipitation, Soil Moisture, and Evapotranspiration Anomalies. Part II: Intraseasonal Drought Intensification Forecasts, *Journal of Hydrometeorology*, 18, 1963–1982, <https://doi.org/10.1175/JHM-D-16-0067.1>, 2017.
- 440 Martens, B., Schumacher, D. L., Wouters, H., Muñoz-Sabater, J., Verhoest, N. E. C., and Miralles, D. G.: Evaluating the surface energy partitioning in ERA5, *Geoscientific Model Development Discussions*, 2020, 1–35, <https://doi.org/10.5194/gmd-2019-315>, 2020.
- Mishra, A. K. and Singh, V. P.: A review of drought concepts, *Journal of Hydrology*, 391, 202–216, <https://doi.org/10.1016/j.jhydrol.2010.07.012>, 2010.
- 445 Moravec, V., Markonis, Y., Rakovec, O., Svoboda, M., Trnka, M., Kumar, R., and Hanel, M.: Europe under multi-year droughts: how severe was the 2014–2018 drought period?, *Environmental Research Letters*, 16, <https://doi.org/10.1088/1748-9326/abe828>, 2021.
- Mueller, B. and Zhang, X.: Causes of drying trends in northern hemispheric land areas in reconstructed soil moisture data, *Climatic Change*, 134, 255–267, <https://doi.org/10.1007/s10584-015-1499-7>, 2016.
- 450 Myneni, R., Knyazikhin, Y., and Park, T.: MODIS/Terra Leaf Area Index/FPAR 8-Day L4 Global 500m SIN Grid V061, <https://doi.org/10.5067/MODIS/MOD15A2H.061>, 2021.



- Naumann, G., Cammalleri, C., Mentaschi, L., and Feyen, L.: Increased economic drought impacts in Europe with anthropogenic warming, *Nature Climate Change*, 11, 485–491, <https://doi.org/10.1038/s41558-021-01044-3>, 2021.
- Otkin, J. A., Svoboda, M., Hunt, E. D., Ford, T. W., Anderson, M. C., Hain, C., and Basara, J. B.: Flash Droughts: A Review and Assessment of the Challenges Imposed by Rapid-Onset Droughts in the United States, *Bulletin of the American Meteorological Society*, 99, 911–919, <https://doi.org/10.1175/BAMS-D-17-0149.1>, 2018.
- Peters, W., Bastos, A., Ciais, P., and Vermeulen, A.: A historical, geographical and ecological perspective on the 2018 European summer drought, *Philosophical Transactions of the Royal Society B: Biological Sciences*, 375, <https://doi.org/10.1098/rstb.2019.0505>, 2020.
- Potapov, P., Li, X., Hernandez-Serna, A., Tyukavina, A., Hansen, M. C., Kommareddy, A., Pickens, A., Turubanova, S., Tang, H., Silva, C. E., Armston, J., Dubayah, R., Blair, J. B., and Hofton, M.: Mapping global forest canopy height through integration of GEDI and Landsat data, *Remote Sensing of Environment*, 253, <https://doi.org/10.1016/j.rse.2020.112165>, 2021.
- Puhe, J.: Growth and development of the root system of Norway spruce (*Picea abies*) in forest stands—a review, *Forest Ecology and Management*, 175, 253–273, [https://doi.org/10.1016/S0378-1127\(02\)00134-2](https://doi.org/10.1016/S0378-1127(02)00134-2), 2003.
- Rakovec, O., Samaniego, L., Hari, V., Markonis, Y., Moravec, V., Thober, S., Hanel, M., and Kumar, R.: The 2018–2020 Multi-Year Drought Sets a New Benchmark in Europe, *Earth's Future*, 10, <https://doi.org/10.1029/2021EF002394>, 2022.
- Reichle, R., De Lannoy, G., Koster, R. D., Crow, W. T., Kimball, J. S., and Liu, Q.: SMAP L4 Global 3-hourly 9 km EASE-Grid Surface and Root Zone Soil Moisture Geophysical Data, Version 6, <https://doi.org/10.5067/08S1A6811J0U>, 2021a.
- Reichle, R., De Lannoy, G., Koster, R. D., Crow, W. T., Kimball, J. S., and Liu, Q.: SMAP L4 Global 3-hourly 9 km EASE-Grid Surface and Root Zone Soil Moisture Geophysical Data, Version 6: User guide, [https://nsidc.org/sites/default/files/multi\\_spl4smau-v006-userguide\\_1\\_0.pdf](https://nsidc.org/sites/default/files/multi_spl4smau-v006-userguide_1_0.pdf), 2021b.
- Richards, L. A.: Capillary conduction of liquids through porous mediums, *Physics*, 1, 318–333, <https://doi.org/10.1063/1.1745010>, 1931.
- Samaniego, L., Thober, S., Wanders, N., Pan, M., Rakovec, O., Sheffield, J., Wood, E. F., Prudhomme, C., Rees, G., Houghton-Carr, H., Fry, M., Smith, K., Watts, G., Hisdal, H., Estrela, T., Buontempo, C., Marx, A., and Kumar, R.: Hydrological Forecasts and Projections for Improved Decision-Making in the Water Sector in Europe, *Bulletin of the American Meteorological Society*, 100, 2451–2472, <https://doi.org/10.1175/BAMS-D-17-0274.1>, 2019.
- Schär, C. and Jendritzky, G.: Hot news from summer 2003, *Nature*, 432, 559–560, <https://doi.org/10.1038/432559a>, 2004.
- Schmidt-Walter, P., Ahrends, B., Mette, T., Puhlmann, H., and Meesenburg, H.: NFIWADS: the water budget, soil moisture, and drought stress indicator database for the German National Forest Inventory (NFI), *Annals of Forest Science*, 76, 39, <https://doi.org/10.1007/s13595-019-0822-2>, 2019.
- Sheffield, J., Wood, E. F., and Roderick, M. L.: Little change in global drought over the past 60 years, *Nature*, 491, 435–438, <https://doi.org/10.1038/nature11575>, 2012.
- Sheffield, J., Wood, E. F., Chaney, N., Guan, K., Sadri, S., Yuan, X., Olang, L., Amani, A., Ali, A., Demuth, S., and Ogallo, L.: A Drought Monitoring and Forecasting System for Sub-Saharan African Water Resources and Food Security, *Bulletin of the American Meteorological Society*, 95, 861–882, <https://doi.org/10.1175/BAMS-D-12-00124.1>, 2014.
- Suárez-Almiñana, S., Pedro-Monzónis, M., Paredes-Arquiola, J., Andreu, J., and Solera, A.: Linking Pan-European data to the local scale for decision making for global change and water scarcity within water resources planning and management, *Science of The Total Environment*, 603–604, 126–139, <https://doi.org/10.1016/j.scitotenv.2017.05.259>, 2017.
- Sutanto, S. J. and Van Lanen, H. A. J.: Catchment memory explains hydrological drought forecast performance, *Scientific Reports*, 12, 2689, <https://doi.org/10.1038/s41598-022-06553-5>, 2022.
- Sutanto, S. J., van der Weert, M., Wanders, N., Blauhut, V., and Van Lanen, H. A. J.: Moving from drought hazard to impact forecasts, *Nature Communications*, 10, 4945, <https://doi.org/10.1038/s41467-019-12840-z>, 2019.
- Svoboda, M., LeComte, D., Hayes, M., Heim, R., Gleason, K., Angel, J., Rippey, B., Tinker, R., Palecki, M., Stooksbury, D., Miskus, D., and Stephens, S.: The drought monitor, *Bulletin of the American Meteorological Society*, 83, 1181–1190, <https://doi.org/10.1175/1520-0477-83.8.1181>, 2002.
- Van Lanen, H. A. J., Laaha, G., Kingston, D. G., Gauster, T., Ionita, M., Vidal, J.-P., Vlnas, R., Tallaksen, L. M., Stahl, K., Hannaford, J., Delus, C., Fendekova, M., Mediero, L., Prudhomme, C., Rets, E., Romanowicz, R. J., Gailliez, S., Wong, W. K., Adler, M.-J., Blauhut, V., Caillouet, L., Chelcea, S., Frolova, N., Gudmundsson, L., Hanel, M., Haslinger, K., Kireeva, M., Osuch, M., Sauquet, E., Stagge, J. H., and Van Loon, A. F.: Hydrology needed to manage droughts: the 2015 European case, *Hydrological Processes*, 30, 3097–3104, <https://doi.org/10.1002/hyp.10838>, 2016.
- Vilhar, U.: Comparison of drought stress indices in beech forests: a modelling study, *iForest - Biogeosciences and Forestry*, 635–642, <https://doi.org/10.3832/ifor1630-008>, 2016.





- 515 Vorobevskii, I.: Global BROOK90 v2.0, [https://github.com/hydrovorobey/Global\\_BROOK90/releases/tag/v2.0](https://github.com/hydrovorobey/Global_BROOK90/releases/tag/v2.0), 2023a.
- Vorobevskii, I.: Supplement materials for publication: Seasonal forecasting of local-scale soil moisture droughts with Global BROOK90., <https://doi.org/10.4211/hs.d882e83bae95438881c7b47f003e7a3c>, 2023b.
- Vorobevskii, I., Kronenberg, R., and Bernhofer, C.: Global BROOK90 R Package: An Automatic Framework to Simulate the Water Balance at Any Location, *Water*, 12, <https://doi.org/10.3390/w12072037>, 2020.
- 520 Vorobevskii, I., Kronenberg, R., and Bernhofer, C.: On the runoff validation of ‘Global BROOK90’ automatic modeling framework, *Hydrology Research*, 52, 1083–1099, <https://doi.org/10.2166/nh.2021.150>, 2021.
- Vorobevskii, I., Luong, T. T., Kronenberg, R., Grünwald, T., and Bernhofer, C.: Modelling evaporation with local, regional and global BROOK90 frameworks: importance of parameterization and forcing, *Hydrology and Earth System Sciences*, 26, 3177–3239, <https://doi.org/10.5194/hess-26-3177-2022>, 2022.
- 525 Wagner, S., Kunstmann, H., Bárdossy, A., Conrad, C., and Colditz, R. R.: Water balance estimation of a poorly gauged catchment in West Africa using dynamically downscaled meteorological fields and remote sensing information, *Physics and Chemistry of the Earth, Parts A/B/C*, 34, 225–235, <https://doi.org/10.1016/j.pce.2008.04.002>, 2009.
- Wanders, N. and Van Lanen, H. A. J.: Future discharge drought across climate regions around the world modelled with a synthetic hydrological modelling approach forced by three general circulation models, *Natural Hazards and Earth System Sciences*, 15, 487–504, <https://doi.org/10.5194/nhess-15-487-2015>, 2015.
- Wanders, N., Karssenber, D., de Roo, A., de Jong, S. M., and Bierkens, M. F. P.: The suitability of remotely sensed soil moisture for improving operational flood forecasting, *Hydrology and Earth System Sciences*, 18, 2343–2357, <https://doi.org/10.5194/hess-18-2343-2014>, 2014.
- 535 Wanders, N., Thober, S., Kumar, R., Pan, M., Sheffield, J., Samaniego, L., and Wood, E. F.: Development and Evaluation of a Pan-European Multimodel Seasonal Hydrological Forecasting System, *Journal of Hydrometeorology*, 20, 99–115, <https://doi.org/10.1175/JHM-D-18-0040.1>, 2019.
- Zappa, M., Bernhard, L., Spirig, C., Pfaundler, M., Stahl, K., Kruse, S., Seidl, I., and Stähli, M.: A prototype platform for water resources monitoring and early recognition of critical droughts in Switzerland, *Proceedings of the International Association of Hydrological Sciences*, 364, 492–498, <https://doi.org/10.5194/piahs-364-492-2014>, 2014.
- 540 Zink, M., Samaniego, L., Kumar, R., Thober, S., Mai, J., Schäfer, D., and Marx, A.: The German drought monitor, *Environmental Research Letters*, 11, <https://doi.org/10.1088/1748-9326/11/7/074002>, 2016.
- Zink, M., Kumar, R., Cuntz, M., and Samaniego, L.: A high-resolution dataset of water fluxes and states for Germany accounting for parametric uncertainty, *Hydrol. Earth Syst. Sci.*, 21, 1769–1790, <https://doi.org/10.5194/hess-21-1769-2017>, 2017.